EP300 and FCGR2B Emerge as Coordinated Mediators of Chromatin-Driven Immune Evasion in Melanoma Resistance

Basma Shabana
Department of Dermatology, Menoufia University, Shebin El-Kom, El-Menoufia, Egypt
Bioinformatics Diploma Program, Nile University, Giza, Egypt
Email: basma.shabana93@gmail.com

Ahmed Salem
Faculty of Medicine, Tanta University, Tanta, Egypt
Email**:** drahmedzakariaanwar@gmail.com

Nouraldeen Ali Ramadan
Neurology and Psychiatry Postgraduate Student, Faculty of Medicine, Ain Shams University, Cairo, Egypt
Email: surgnour@gmail.com

Ahmed Mahmoud Khedr
Cardiology and Vascular Medicine Postgraduate Student, Faculty of Medicine, Ain Shams University, Cairo, Egypt
Email**:** cardiologistahmedkhedr@gmail.com

Corresponding author: Basma Shabana
(Email: basma.shabana93@gmail.com)

Abstract:

Immune checkpoint inhibitors targeting PD-1 have significantly improved outcomes in metastatic melanoma, yet 40–60% of patients exhibit primary resistance. While tumor-intrinsic epigenetic dysregulation has been implicated, its interplay with immune evasion remains poorly defined. In this study, we analyzed RNA-seq data from the GSE168204 dataset (n = 25 pre/on-treatment biopsies) comparing responders (n = 9) and non-responders (n = 16) to anti-PD-1 therapy. Using DESeq2 (|log2FC| > 1.5, padj < 0.05), we identified key differentially expressed genes (DEGs) in non-responders, including chromatin remodelers SMARCA2 (log2FC = 1.63, padj = 0.005) and KAT6B (log2FC = 2.8, padj = 1.2e-08), and the inhibitory receptor FCGR2B (log2FC = 2.196, padj = 0.001). Functional enrichment and protein–protein interaction analysis highlighted EP300 and KMT2A as hub genes linking histone acetylation (GO:0000123) to extracellular matrix remodeling (KEGG:04512). Transcription factor analysis identified STAT3 and RELA as central regulators of this resistance signature. These findings suggest that non-responder melanomas coordinately upregulate chromatin modifiers and immune checkpoints, promoting immune evasion. Our results nominate EP300 and FCGR2B as potential therapeutic targets to overcome resistance, warranting preclinical validation.

Keywords:

Anti-PD-1 resistance melanoma ; SMARCA2; EP300; FCGR2B; Chromatin remodeling; Epigenetic regulation; Tumor microenvironment

Introduction:

Immunotherapy Resistance in Melanoma: The Unmet Challenge

Immune checkpoint inhibitors (ICIs) targeting PD-1 have revolutionized metastatic melanoma treatment, with 40–50% of patients achieving durable responses [3]. However, primary resistance remains a major clinical hurdle, with over half of patients deriving no benefit [4]. While tumor mutational burden (TMB) and PD-L1 expression partially predict response, recent evidence implicates **epigenetic reprogramming** as a key mediator of immune evasion [9]. Specifically, chromatin remodelers (e.g., SWI/SNF complexes) can silence interferon signaling and antigen presentation [5], but their interplay with inhibitory immune receptors (e.g., FCGR2B) is poorly understood.

The Epigenetic-Immune Axis in Resistance

Chromatin regulators like EP300 and KMT2A modulate PD-1 response in other cancers [6] yet their role in melanoma remains undefined. Concurrently, non-responders often exhibit upregulated immune checkpoints beyond PD-L1, including LAG3 and TIGIT [13]. Intriguingly, FCGR2B—an inhibitory Fcγ receptor—was recently linked to macrophage-mediated immunosuppression in melanoma [2], but its association with epigenetic dysregulation has not been explored.

Materials and Methods:

Dataset Acquisition and Preprocessing

RNA-seq data were obtained from the **Gene Expression Omnibus (GEO)** under accession number **GSE168204**, comprising transcriptomic profiles from 25 metastatic melanoma tumor biopsies, including pre-treatment (n = 10) and on-treatment (n = 15) samples. Patients were classified into **responders (R; n = 9)** and **non-responders (NR; n = 16)** based on clinical response criteria.

Sample distribution:

- Pre-treatment: 5 NR, 5 R
- On-treatment: 11 NR, 4 R

Quality control was performed using **edgeR**, with genes expressed at <10 counts across all samples filtered out. All analyses were conducted in **R (v4.3.2 "Eye Holes")** on a Windows UCRT platform.

Differential Expression Analysis

Differential gene expression was assessed using the **DESeq2** package (v1.42.1) [11], with default settings. Genes were considered significantly differentially expressed if they satisfied the thresholds:
|log□FC| > 1.5 and **adjusted p-value (padj) < 0.05** using the **Benjamini–Hochberg** correction.

Functional Enrichment Analysis

Functional enrichment of upregulated genes in non-responders was performed to identify enriched biological terms and pathways.

Tools and databases used:

- **Gene Ontology (GO)**: Biological Process (BP), Molecular Function (MF), Cellular Component (CC) annotations were analyzed using **clusterProfiler** (v4.10.1).
- **Pathway enrichment**: KEGG and Reactome terms were identified using the **ReactomePA** package (v1.46.0).

Significance criteria: Terms with **p.adjust < 0.05** and **q-value < 0.2** were retained.

Protein–Protein Interaction (PPI) Network Construction

PPI data were retrieved from the **STRING database** (version 12) [16] via the **STRINGdb** R package. Genes were mapped to STRING identifiers, and interactions with a **confidence score > 400** (medium-to-high confidence) were retained. Networks were visualized in **Cytoscape (v3.9.1)**, and **hub genes** were prioritized based on **degree centrality**. Cluster detection within the PPI network was performed using the **MCODE** plugin.

Transcription Factor and Receptor Annotation

Transcription factors regulating upregulated DEGs were identified using **TRRUST v2** [7]. Receptor annotations were derived from curated gene sets and analyzed using **OmnipathR** (v3.10.1), which also enabled mapping of **receptor–TF regulatory interactions**.

Results:

Differential Gene Expression Analysis Between Responders and Non-Responders

To uncover transcriptional differences associated with anti-PD-1 therapy response, we performed differential gene expression analysis between responders (R) and non-responders (NR) using **DESeq2**. A total of **4,536 differentially expressed genes (DEGs)** were identified based on an adjusted p-value < 0.05 and an absolute log□ fold change > 1.5. Of these, **2,863 genes were upregulated** and **1,673 were downregulated** in non-responders relative to responders.

Key Upregulated Genes in Non-Responders:

- **Chromatin remodelers:**
  - *SMARCA2* (log□FC = 1.63, padj = 0.005)
  - *KAT6B* (log□FC = 2.8, padj = 1.2e-08)
- **Immune checkpoint regulator:**
  - *FCGR2B* (log□FC = 2.196, padj = 0.001)
- **Extracellular matrix component:**
  - *COL1A1* (log□FC = 3.9, padj = 1.8e-06)

A summary of selected DEGs is provided in **Table 1**, while the complete list is available in the **Supplementary Files**. The overall distribution of DEGs is visualized in **Figure 1 (volcano plot)**, highlighting significantly upregulated (left) and downregulated (right) genes in the non-responder group. Cluster analysis of the **top 30 DEGs** is shown in **Figure 2**, which illustrates clear expression-based separation between responders and non-responders.

Functional Enrichment Analysis of Differentially Expressed Genes (DEGs):

Functional enrichment analysis of the upregulated genes in non-responders revealed significant associations with pathways related to chromatin remodeling, immune signaling, and extracellular matrix dynamics (Figures 3–7).

Gene Ontology (GO) Enrichment

- **Biological Processes (GO-BP):** The most significantly enriched terms included *nucleosome assembly* (GO:0006334, padj = 1.8e−16) and *extracellular matrix (ECM) organization* (GO:0030198, padj = 0.0008), indicating coordinated chromatin and structural remodeling in resistant tumors (**Figure 3**).
- **Molecular Functions (GO-MF):** Enriched functions included *structural constituent of chromatin* (GO:0030527, padj = 9.9e−42), *GTPase activator activity*, and *ECM structural constituents* (GO:0005201, padj = 3.3e−14), highlighting the role of nuclear and matrix architecture in immune evasion (**Figure 4**).
- **Cellular Components (GO-CC):** Top enriched terms included *nucleosome* (GO:0000786, padj = 3.9e−30), *CENP-A-containing chromatin*, and the *voltage-gated calcium channel complex* (GO:0005891, padj = 3.6e−06) (**Figure 5**).

Pathway Enrichment

- **KEGG Pathways:** Upregulated genes were enriched in immune and cancer-related pathways, including *systemic lupus erythematosus* (hsa05322, padj = 3.3e−29), *neutrophil extracellular trap formation* (hsa04613, padj = 1.7e−24), *microRNAs in cancer* (hsa05206, padj = 2.3e−05), *ECM–receptor interaction* (hsa04512, padj = 2.3e−05), *calcium signaling pathway* (hsa04020, padj = 0.036), and *viral carcinogenesis* (hsa05203, padj = 2.3e−05) (**Figure 6**).
- **Reactome Pathways:** Significant pathways included *chromatin modification* (R-HSA-4839726, padj = 1.1e−21), *histone deacetylation* (R-HSA-3214815, padj = 1.7e−36), *RNA polymerase I promoter opening* (R-HSA-73728, padj = 9.9e−40), *RUNX1 regulation of megakaryocyte differentiation* (R-HSA-8936459, padj = 1.5e−37), *granulopoiesis regulation* (R-HSA-9616222, padj = 2.1e−37), and *NOTCH signaling* (R-HSA-157118, padj = 5.7e−14) (**Figure 7**).

These results highlight extensive alterations in chromatin structure, immune function, and ECM signaling in anti-PD-1-resistant melanomas, suggesting that transcriptional rewiring and microenvironmental remodeling contribute to immune escape.

Protein–Protein Interaction (PPI) Network and Hub Gene Analysis:

A protein–protein interaction (PPI) network was constructed using the STRING database (version 12) based on significantly upregulated genes in non-responders. The resulting interaction map was imported into Cytoscape for visualization, with node attributes scaled by log□ fold change values. The network revealed a densely connected cluster of histone variants and transcriptional regulators, suggesting coordinated epigenetic remodeling in non-responders.

Hub genes were identified based on interaction degree, with the top 20 listed in **Table 2** (full list available in the Supplementary Files), and the primary interaction cluster visualized in **Figure 8**. Notable hub genes included multiple histone variants (e.g., **H3C12, H3C13, H2BC4, H2BC11**), as well as epigenetic regulators such as **EP300** (degree = 252), **CREBBP**, **KMT2A** (degree = 206), and **KDM6A**. Several immune-related genes also emerged as hubs, including **PTEN**, **TLR4**, and **PTPRC**. The high connectivity and upregulation of EP300 and KMT2A—key transcriptional co-activators—suggest their potential role in rewiring transcriptional control within the tumor microenvironment.

The full network was exported as a Cytoscape-compatible CSV file, containing both node and edge attributes, to support further annotation and exploration. To identify functional gene modules, **MCODE** clustering was applied, revealing 41 distinct

clusters enriched for biological processes including chromatin remodeling, immune signaling, and inflammatory response. **Figure 8** displays the top-ranked cluster identified through this analysis.

Transcription Factors (TFs) and Receptor Enrichment in Upregulated Genes of Non-Responders:

To explore the regulatory mechanisms underlying gene expression changes in non-responders, we analyzed transcription factor (TF) enrichment and upstream modulators, including receptors and chromatin regulators, associated with the upregulated genes.

Transcription Factor Enrichment

Using the **TRRUST database**, we identified key TFs that are likely to regulate the upregulated genes in non-responders. The most enriched transcription factors included **SP1**, **NFKB1**, **RELA (NF-κB)**, **SP3**, **STAT3**, **TP53**, **ETS1**, and **YY1**. These TFs are widely recognized for their roles in inflammation, immune evasion, and cell proliferation—hallmarks of resistance to anti-PD-1 therapy.
Figure 9 displays a bar plot of the top 10 enriched TFs.

To further understand regulatory connectivity, we constructed a **TF–target gene network** that maps the direct relationships between the top 20 enriched TFs and their downstream targets. **Figure 10** presents this regulatory network.

Upstream Modulators of Transcription Factors

Using the **OmniPath** database, we identified upstream modulators—both classical surface receptors (e.g., **DDR1**, **PTPRC**) and chromatin-associated regulators (e.g., **EP300**, **KDM6A**)—that may influence TF activity through intracellular

signaling or epigenetic modification. The top 20 modulators included:
EP300, **EGR1**, **FOXA1**, **TAF1**, **EBF1**, **TCF12**, **TCF4**, **ZEB1**, **CHD2**, **NANOG**, **FOXP1**, **BDP1**, **POU5F1**, **MYCN**, **PRDM1**, **WT1**, **PGR**, **TCF7L2**, **KDM6A**, **NFIA**, **E2F1**.

Notably:

- **EP300 acetylates STAT3 at lysine 685**, enhancing its transcriptional activity [3].
- **EP300 also acetylates RELA (NF-κB)**, promoting its transcriptional function [4].

Figure 11 shows the top 10 receptors ranked by the number of transcription factors they regulate.
Figure 12 presents the full receptor–TF interaction network for the top 20 receptor candidates.

Ligand–Receptor Interactions

To uncover upstream extracellular signals, we investigated ligand–receptor interactions influencing the identified pathways. A key interaction pair included **COL1A1 (ligand)** and **DDR1 (receptor)**. DDR1-mediated collagen signaling has been shown to promote immune evasion by forming physical collagen barriers that exclude T cells from the tumor microenvironment [9].
Figure 13 illustrates the ligand–receptor interaction network involving the top 20 ligands identified.

Discussion

Our study uncovers a coordinated epigenetic–immune program underlying resistance to PD-1 blockade in metastatic melanoma. Three major findings emerge:

---

1. Chromatin Remodeling Establishes an Immune-Suppressive Niche

We identified **SMARCA2** (log□FC = 1.63) and **KAT6B** (log□FC = 2.8) as chromatin remodelers significantly upregulated in non-responders. These genes regulate **nucleosome repositioning** (GO:0006334) and **histone acetylation** (GO:0016573), supporting previous reports that **SWI/SNF complexes** contribute to immune evasion by silencing interferon-stimulated genes in melanoma [1]. Although direct spatial transcriptomic evidence in melanoma is limited, studies in other solid tumors, such as lung cancer, have linked **SMARCA2 dysregulation** with altered **CD8□ T-cell infiltration** and immune evasion [12], suggesting that similar mechanisms may contribute to immune exclusion in melanoma.

Protein–protein interaction (PPI) analysis further highlighted **EP300**, a transcriptional coactivator, as a central node connecting chromatin remodeling to immune regulatory pathways. EP300 is known to **acetylate key transcription factors** such as **STAT3** and **RELA (NF-κB)** at specific lysine residues, thereby enhancing their transcriptional activity and promoting the expression of immunosuppressive genes [19,14]. Acetylation of RELA at **lysine 310**, in particular, is critical for full NF-κB activation. In preclinical models of lung adenocarcinoma, **EP300 inhibition** restored sensitivity to PD-1 blockade [17], suggesting that targeting chromatin remodeling could reprogram the tumor immune microenvironment to improve response to immunotherapy.

---

2. FCGR2B Emerges as a Co-opted Immune Checkpoint

We observed significant upregulation of **FCGR2B** (log□FC = 2.96), an inhibitory Fcγ receptor, in non-responders. FCGR2B is implicated in **macrophage-mediated immunosuppression** and **T-cell inhibition** through engagement with IgG-opsonized targets [2]. Our transcription factor enrichment analysis identified **RELA (NF-κB)** as one of the most enriched TFs in non-responders. While direct transcriptional regulation of **FCGR2B by RELA** has been documented in B cells [18], its relevance in melanoma remains to be validated. RELA activity may be further amplified by **EP300-mediated acetylation**, forming a potential **feedforward loop** in which EP300 enhances RELA's transcriptional output, including the upregulation of immunosuppressive targets such as FCGR2B.

Although **FCGR2B** has been the focus of early-phase clinical trials in hematologic malignancies (e.g., NCT04502394), its potential as an immune checkpoint in solid tumors like melanoma remains underexplored. These findings suggest that FCGR2B may serve as a **novel immunotherapeutic target** in resistant disease.

---

3. Therapeutic Opportunities Beyond PD-1 Blockade

The convergence of **epigenetic regulation** (e.g., EP300, KMT2A) and **immune inhibition** (e.g., FCGR2B) highlights dual therapeutic vulnerabilities in PD-1-resistant melanoma. First, **epigenetic priming** with **histone acetyltransferase inhibitors** such as **A485** could promote chromatin accessibility, thereby enhancing antigen presentation and interferon signaling [8]. Second, **dual immune checkpoint blockade**, targeting both **PD-1 and FCGR2B**, may help to overcome resistance driven by macrophage- and B-cell-mediated immunosuppression.

Additionally, our analysis revealed **ligand–receptor interactions**—notably **COL1A1–DDR1**—suggesting that

stromal remodeling may contribute to T-cell exclusion[15]. This observation is supported by work from **Junquan Liu,.et al,** who demonstrated that **DDR1 inhibition** disrupts collagen alignment and improves T-cell infiltration in solid tumors [10].

Together, these results present a **systems-level framework** in which chromatin remodeling, immune checkpoints, and stromal signaling converge to sustain immune resistance in melanoma. These findings warrant further experimental validation and may guide future combination therapy strategies to overcome immune checkpoint blockade resistance.

Limitations and Future Directions

While our findings uncover novel insights into mechanisms of resistance to PD-1 blockade in melanoma, several limitations must be acknowledged:

Cohort Size Constraints

Our analysis was limited to a relatively small cohort of 25 patient samples (16 non-responders, 9 responders), which may not capture the full heterogeneity of resistance mechanisms. Larger, independent validation cohorts are required to confirm the generalizability of our findings.

Limitations of Bulk RNA-Sequencing

Bulk RNA-seq provides an average transcriptomic signal across all cell types, precluding cell-type-specific resolution. As such, we cannot determine:

- Whether the observed upregulation of chromatin remodelers (e.g., *SMARCA2*, *KAT6B*) originates from tumor cells versus stromal or immune components.
- Whether *EP300* activity is intrinsic to melanoma cells or derived from tumor-associated macrophages (TAMs).
- Whether *FCGR2B* expression reflects increased B-cell infiltration or melanoma-intrinsic expression.

These questions could be addressed through **single-cell RNA-sequencing (scRNA-seq)** of pre-treatment tumor biopsies.

Lack of Spatial Context

Our study lacks spatial transcriptomic data, which limits our ability to:

- Visualize patterns of **CD8 T-cell exclusion** in *SMARCA2*-high tumor regions.
- Confirm the spatial co-localization of **DDR1, COL1A1**, and immune cells.

These gaps could be addressed by:

- **Multiplex immunohistochemistry (IHC)** co-staining DDR1, CD8, and COL1A1.
- **Spatial transcriptomics platforms** (e.g., 10x Genomics Visium) to map stromal–immune interfaces.

Lack of Mechanistic Validation

Our proposed regulatory model—wherein *EP300* acetylates *STAT3* (K685) and *RELA* (K310) to drive *FCGR2B* expression, and *SMARCA2* mediates chromatin compaction to silence interferon signaling—remains hypothetical. Validation is needed through:

- **ChIP-seq** to confirm RELA binding at the *FCGR2B* promoter in melanoma cells.
- **In vitro functional assays** to measure STAT3 acetylation and target gene expression following EP300 inhibition.

Strategic Future Directions

To address these limitations and validate therapeutic hypotheses, we propose:

Functional Studies

- Test **EP300 inhibitors (e.g., A485)** in combination with **anti-FCGR2B antibodies** using:
  - **Patient-derived organoids (PDOs)** engineered to overexpress *SMARCA2*.
  - **NSG mouse models** engrafted with tumors from non-responder patients.

Multi-Omic Integration

- Incorporate **ATAC-seq** to define chromatin accessibility changes in non-responders versus responders.
- Use **quantitative proteomics** to measure *STAT3* and *RELA* acetylation levels across patient samples.

References

1. Esteller, M. et al., 2024. The Epigenetic Hallmarks of Cancer. *Cancer Discovery*, 14(10), pp.1783-1809. https://doi.org/10.1158/2159-8290.CD-24-0296

2. Farley, C.R. et al., 2021. FcγRIIB is a T cell checkpoint in antitumor immunity. *JCI Insight*, 6(4), e135623. https://doi.org/10.1172/jci.insight.135623

3. Gellrich, F.F. et al., 2020. Anti-PD-1 and novel combinations in the treatment of melanoma. *Journal of Clinical Medicine*, 9(1), p.223. https://doi.org/10.3390/jcm9010223

4. Gide, T.N. et al., 2018. Primary and acquired resistance to immune checkpoint inhibitors in cancer. *Clinical Cancer Research*, 24(6), pp.1260-1270. https://doi.org/10.1158/1078-0432.CCR-17-2267

5. Grasso, C.S. et al., 2020. Conserved interferon-γ signaling drives clinical response to immune checkpoint blockade therapy in melanoma. *Cancer Cell*, 38(4), pp.500-515.e3. https://doi.org/10.1016/j.ccell.2020.08.005

6. Gronkowska, K. et al., 2024. Genetic dysregulation of EP300 in cancers in light of cancer epigenome control. *Molecular Therapy: Oncology*, 32(4), p.200871. https://doi.org/10.1016/j.omton.2024.200871

7. Han, H. et al., 2018. TRRUST v2: an expanded reference database of human and mouse transcriptional regulatory interactions. *Nucleic Acids Research*, 46(D1), pp.D380-D386. https://doi.org/10.1093/nar/gkx1013

8. Jaschke, N.P. et al., 2024. Small-molecule CBP/p300 histone acetyltransferase inhibition mobilizes leukocytes from the bone marrow via the endocrine stress response. *Immunity*, 75(2), pp.364-378.e9. https://doi.org/10.1016/j.immuni.2024.01.005

9. Joo, H. et al., 2025. Epigenetic mechanisms in melanoma development and progression. *Trends in Cancer*. https://doi.org/10.1016/j.trecan.2025.04.007

10. Liu, J. et al., 2023. A highly selective humanized DDR1 mAb reverses immune exclusion by disrupting collagen fiber alignment in breast cancer. *Journal for ImmunoTherapy of Cancer*, 11, e006720. https://doi.org/10.1136/jitc-2023-006720

11. Love, M.I. et al., 2014. Moderated estimation of fold change and dispersion for RNA-seq data with DESeq2. *Genome Biology*, 15, p.550. https://doi.org/10.1186/s13059-014-0550-8

12. Park, L.C. et al., 2018. Impact of Chromatin Remodeling Genes Including SMARCA2 and PBRM1 on Neoantigen and Immune Landscape of NSCLC. *Journal of Thoracic*

Oncology, 13(10), p.S525. https://doi.org/10.1016/j.jtho.2018.08.716

13. Sade-Feldman, M. et al., 2018. Defining T cell states associated with response to checkpoint immunotherapy in melanoma. *Cell*, 175(4), pp.998-1013.e20. https://doi.org/10.1016/j.cell.2018.10.038

14. Sim, D.Y. et al., 2019. Suppression of STAT3 Phosphorylation and RelA/p65 Acetylation Mediated by MicroRNA134 Plays a Pivotal Role in the Apoptotic Effect of Lambertianic Acid. *International Journal of Molecular Sciences*, 20(12), p.2993. https://doi.org/10.3390/ijms20122993

15. Sun, X. et al., 2021. Tumour DDR1 promotes collagen fibre alignment to instigate immune exclusion. *Nature*, 599, pp.673-678. https://doi.org/10.1038/s41586-021-04057-2

16. Szklarczyk, D. et al., 2021. The STRING database in 2021: customizable protein-protein networks, and functional characterization of user-uploaded gene/measurement sets. *Nucleic Acids Research*, 49(D1), pp.D605-D612. https://doi.org/10.1093/nar/gkaa1074

17. Xia, Z. et al., 2024. EP300 restores the glycolytic activity and anti-tumor function of CD8+ cytotoxic T cells in nasopharyngeal carcinoma. *iScience*, 27(2), p.108957. https://doi.org/10.1016/j.isci.2024.108957

18. Xiu, Y. et al., 2002. Transcriptional Regulation of Fcgr2b Gene by Polymorphic Promoter Region and Its Contribution to Humoral Immune Responses. *The Journal of Immunology*, 169(8), pp.4340-4346. https://doi.org/10.4049/jimmunol.169.8.4340

19. Yu, H. et al., 2009. STATs in cancer inflammation and immunity: a leading role for STAT3. *Nature Reviews Cancer*, 9, pp.798-809. https://doi.org/10.1038/nrc2734

(Table 1)

GeneID	baseMean	log2FoldChange	lfcSE	stat	pvalue	padj
100302278	1.57693524494273	3.43127134716989	1.1862536717925	2.8925274 8274746	0.0038215574 6591999	0.0202379255757 06
645520	2.23944959013747	4.21060265719893	0.9473178 07172052	4.4447624 9187006	8.7989018329519e-06	0.0001675179572 47477
729737	1186.16600607583	1.85701081996872	0.6571129 01260041	2.8260148 5438473	0.0047131078 3621156	0.0235264089799799
729759	17.4137493071576	7.25548513179509	1.4858341 0358219	4.8831058 0185424	1.0442780113 8992e-06	2.8150463432866 3e-05
81399	28.0353538737398	4.57582164397408	0.7542216 8108519	6.0669452 4796845	1.3036597432185e-09	8.4686935687053 9e-08
107984841	143.793072768933	2.58085109444073	0.6037736 14756466	4.2745344 1383278	1.9153712057 4941e-05	0.0003190659353 44339
107984847	227.761099053972	2.97416657393554	0.5919365 37519034	5.0244686 4726593	5.0482825969061e-07	1.5240851455488 5e-05
107984849	29.9915565811509	1.87648194262128	0.6857606 22151437	2.7363512 6020242	0.0062124672 7751893	0.0290565612733321
105378580	53.5579164326631	1.91089120865553	0.4149700 58002552	4.6048893 6925607	4.1268519012 3527e-06	8.9774119341883 2e-05
284593	5.68788537259092	-1.813902181	0.6566627 29958398	-2.762304145	0.0057394985 2306079	0.0273317743957957
8511	122.765713379762	2.77730402711752	0.5228875 09705936	5.3114751 7499401	1.0874138553 8976e-07	4.1580704635458 5e-06
105378949	17.6310829541834	-2.711349283	0.7099080 31540787	-3.819296532	0.0001338328 00336688	0.0015194243760 2014
8764	11730.6531669402	-1.535702345	0.5103829 36594115	-3.008921801	0.0026217658 7701715	0.0152471414185533
388588	160.009303845045	-2.601339454	0.5582064 42638038	-4.660174544	3.1594135219 2875e-06	7.1537425723287 4e-05
100133612	8.23711512848261	-2.030196196	0.7699813 0153979	-2.636682465	0.0083721160 4286078	0.0361244854388 7
105376673	9.74163931365781	-4.644403908	1.6538358 2298518	-2.808261766	0.0049809721 0699313	0.0245341310439972
284661	3.58654767744336	-4.720467419	1.6242485 616837	-2.906246944	0.0036579264 0322053	0.0195953903890437
55966	409.922172549919	-3.912070848	0.8565240 99869991	-4.567379772	4.9385876839077e-06	0.0001043807730 15424
148645	20.5201487764738	-2.785372857	0.8869584 67096289	-3.140364471	0.0016873776 2114787	0.0108318756970 46
387509	2546.12424469508	-2.280234353	0.5994123 85728159	-3.8041161	0.0001423113 83013126	0.0015996161739 0013

				77		

Table (2)

STRING_id	GeneSymbol	Degree	log2FoldChange
ENSP00000346839	FN1	310	-1.957673251
ENSP00000352252	H3C12	278	-2.515948088
ENSP00000333277	H3C13	272	-5.354650119
ENSP00000263253	EP300	252	-2.313545877
ENSP00000244537	H4C6	248	-7.739781464
ENSP00000355657	H3-4	246	-4.692499087
ENSP00000411355	PTPRC	224	-2.190052752
ENSP00000332194	H2AC20	214	-4.470291901
ENSP00000262367	CREBBP	212	-1.979801064
ENSP00000358155	H2AC18	210	-3.269413113
ENSP00000361021	PTEN	206	-1.523926192
ENSP00000436786	KMT2A	206	-2.748972172
ENSP00000321744	H2BC4	194	-4.11423315
ENSP00000363089	TLR4	194	-1.9621741
ENSP00000289316	H2BC5	190	-2.100870263
ENSP00000477527	H2BC17	190	-3.642363024
ENSP00000482674	H2BC3	190	-6.494513763
ENSP00000367203	KDM6A	188	-1.746178128
ENSP00000476136	H2BC11	188	-4.09081271
ENSP00000479169	H2BC9	188	-5.76814074

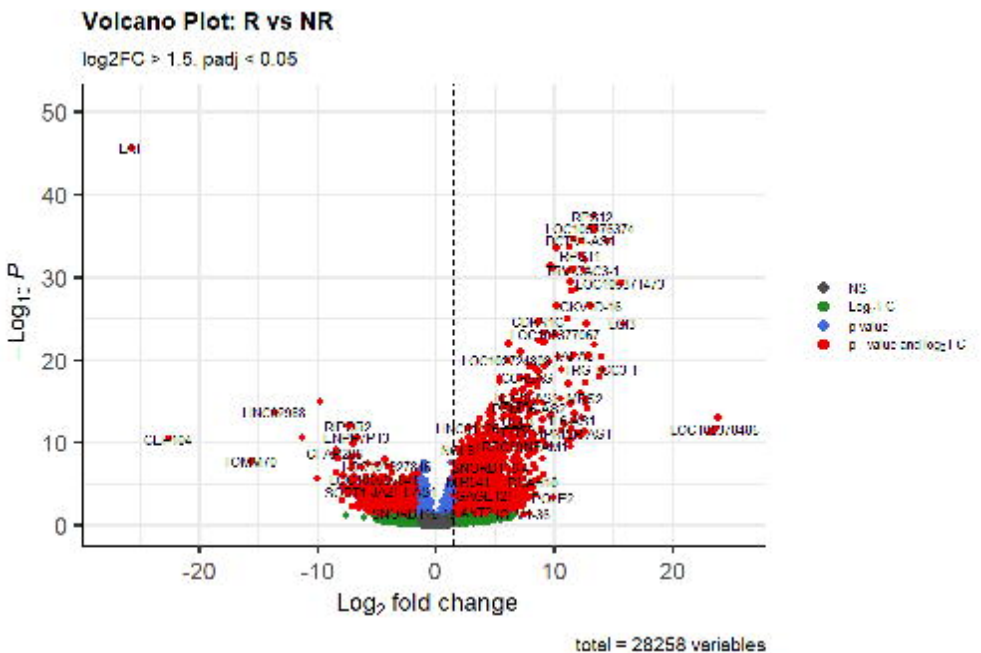
Volcano Plot: R vs NR
log2FC > 1.5, padj < 0.05
−Log10 P
Log2 fold change
NS
Log2 FC
p value
p value and log2 FC
total = 28258 variables

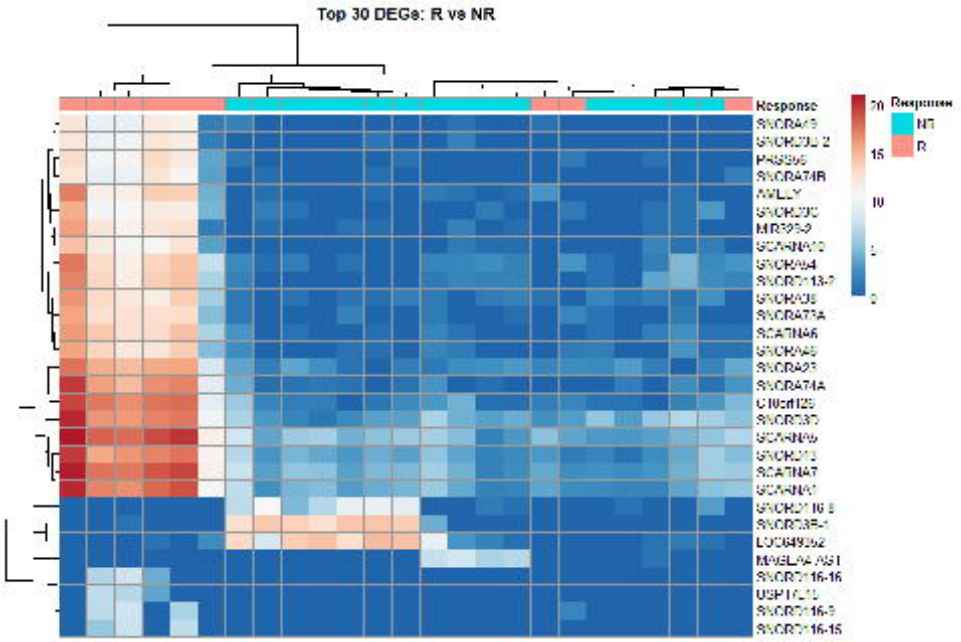
Top 30 DEGs: R vs NR
Response
NR
R
20
15
10
5
0

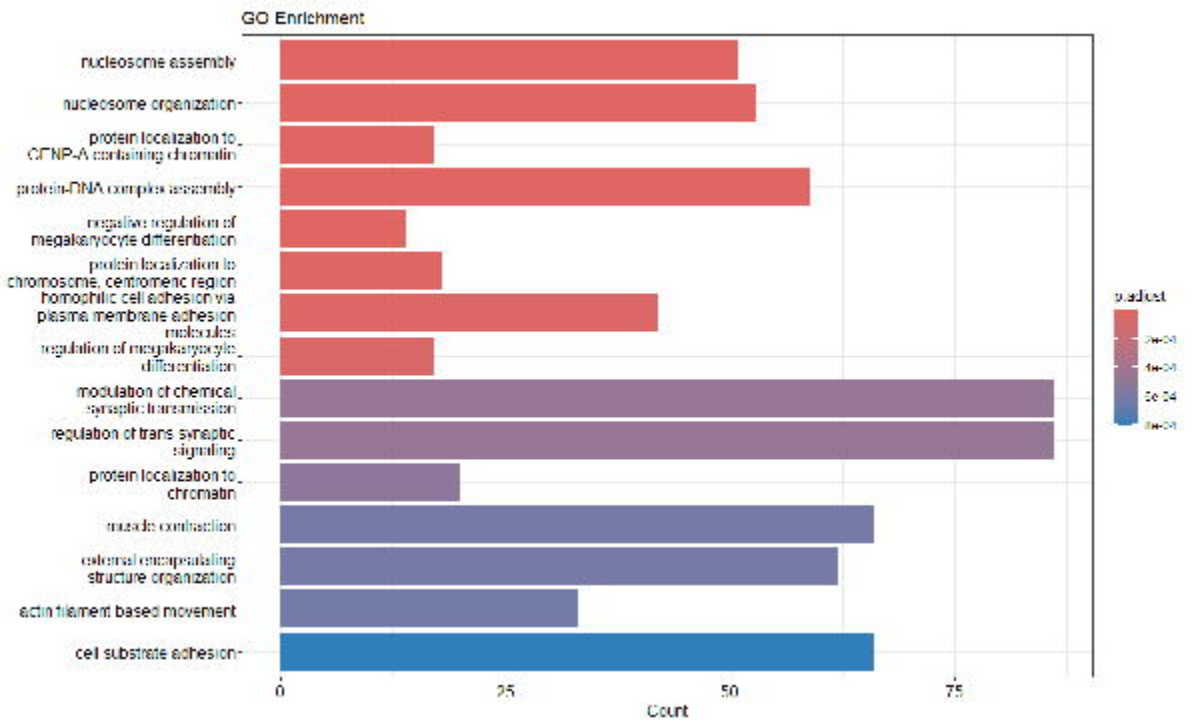
GO Enrichment
nucleosome assembly
nucleosome organization
protein localization to CENP-A containing chromatin
protein-DNA complex assembly
negative regulation of megakaryocyte differentiation
protein localization to chromosome, centromeric region
homophilic cell adhesion via plasma membrane adhesion molecules
regulation of megakaryocyte differentiation
modulation of chemical synaptic transmission
regulation of trans synaptic signaling
protein localization to chromatin
muscle contraction
external encapsulating structure organization
actin filament based movement
cell substrate adhesion
0
25
50
75
Count
p.adjust

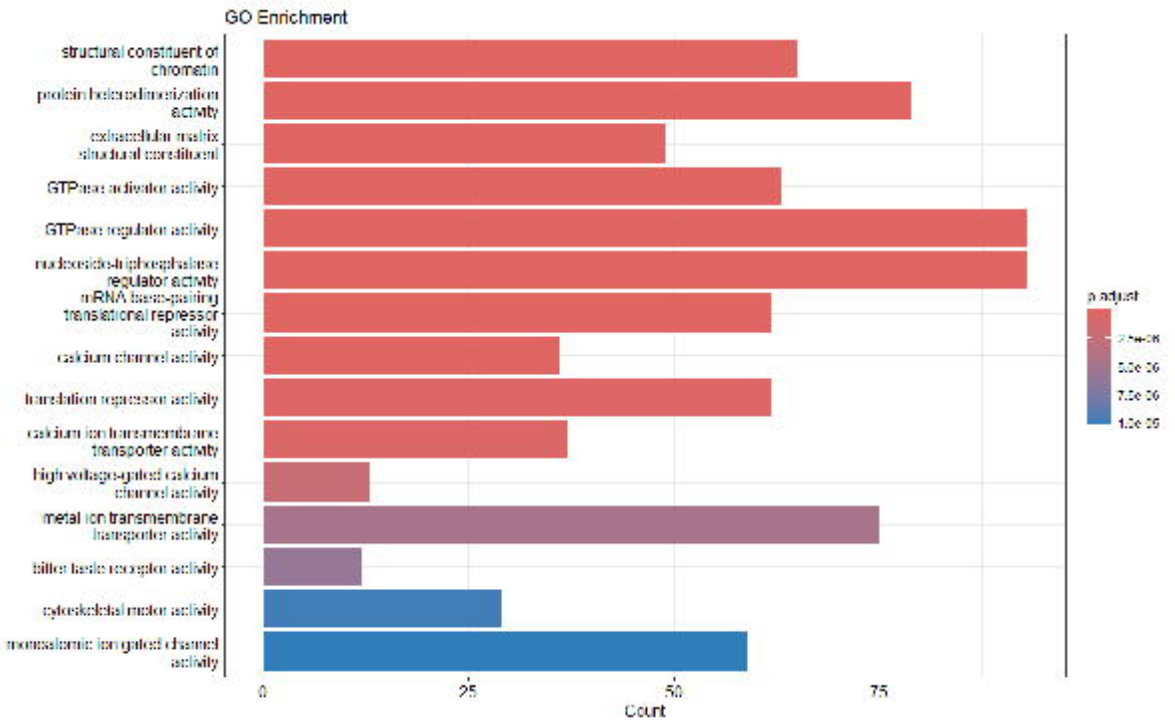
GO Enrichment
structural constituent of chromatin
protein heterodimerization activity
extracellular matrix structural constituent
GTPase activator activity
GTPase regulator activity
nucleoside-triphosphatase regulator activity
mRNA base-pairing translational repressor activity
calcium channel activity
translation repressor activity
calcium ion transmembrane transporter activity
high voltage-gated calcium channel activity
metal ion transmembrane transporter activity
bitter taste receptor activity
cytoskeletal motor activity
monoatomic ion gated channel activity
0
25
50
75
Count
p.adjust
5.0e-06
7.5e-06
1.0e-05

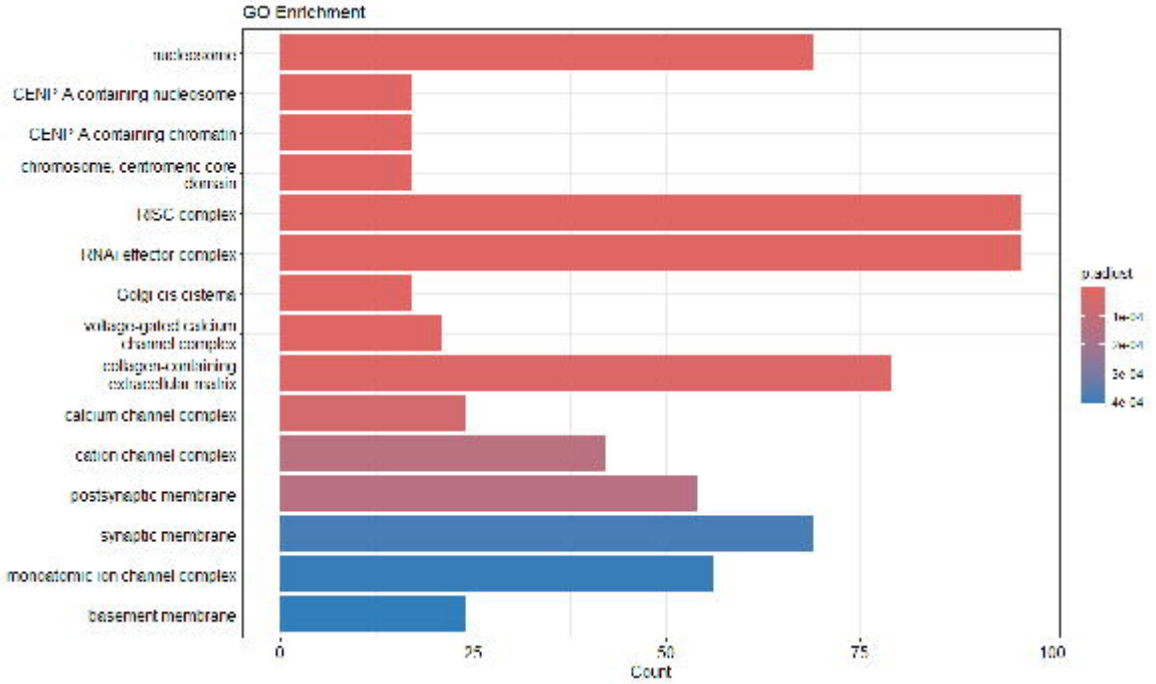
GO Enrichment
nucleosome
CENP-A containing nucleosome
CENP-A containing chromatin
chromosome, centromeric core domain
RISC complex
RNAi effector complex
Golgi cis cisterna
voltage-gated calcium channel complex
collagen-containing extracellular matrix
calcium channel complex
cation channel complex
postsynaptic membrane
synaptic membrane
monoatomic ion channel complex
basement membrane
0
25
50
75
100
Count
p.adjust
1e-24
2e-24
3e-24
4e-24

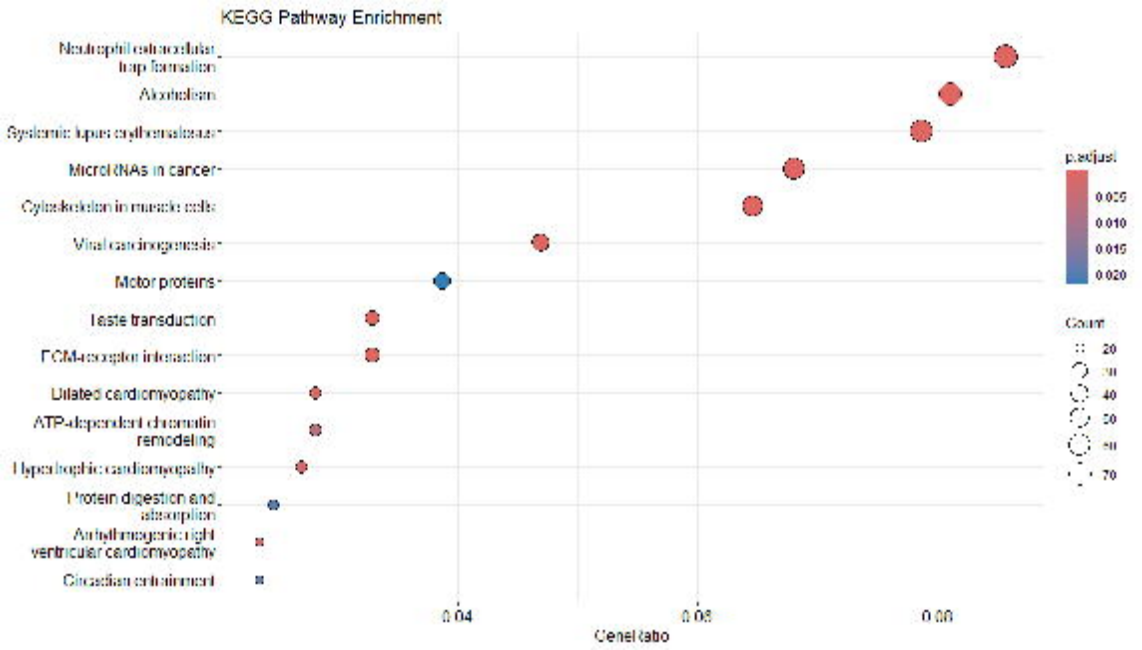
KEGG Pathway Enrichment
Neutrophil extracellular trap formation
Alcoholism
Systemic lupus erythematosus
MicroRNAs in cancer
Cytoskeleton in muscle cells
Viral carcinogenesis
Motor proteins
Taste transduction
ECM-receptor interaction
Dilated cardiomyopathy
ATP-dependent chromatin remodeling
Hypertrophic cardiomyopathy
Protein digestion and absorption
Arrhythmogenic right ventricular cardiomyopathy
Circadian entrainment
0.04
0.08
0.00
GeneRatio
p.adjust
0.025
0.020
0.015
0.010
0.020
Count
20
30
40
50
60
70

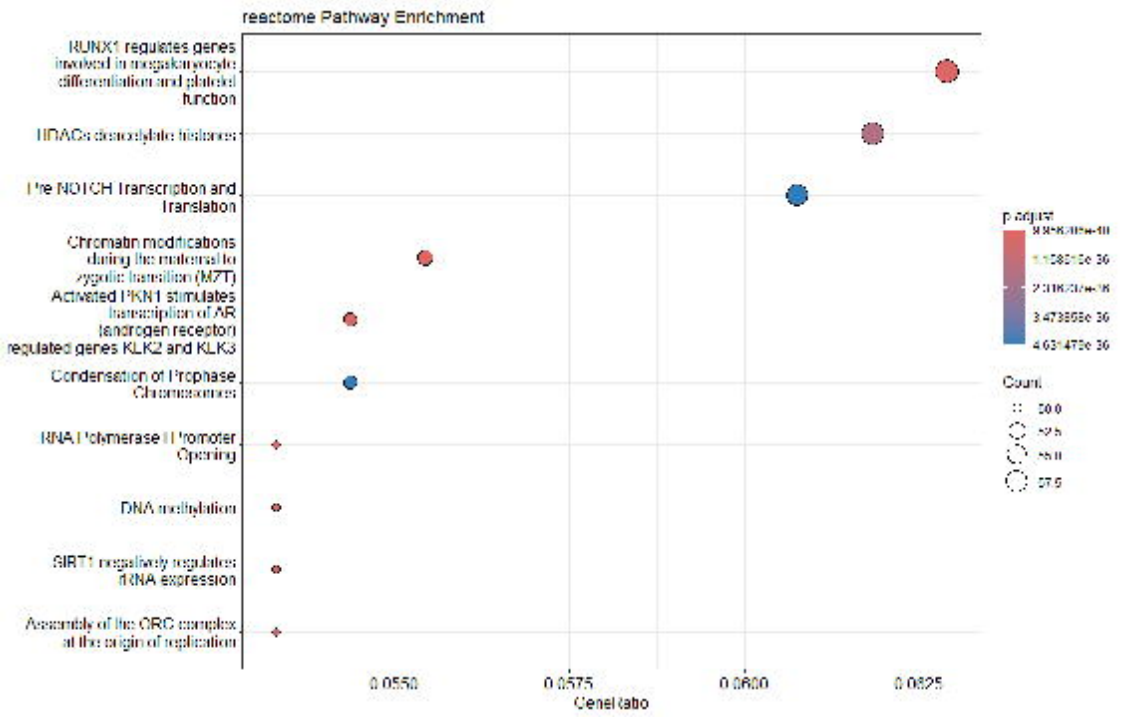
reactome Pathway Enrichment
RUNX1 regulates genes involved in megakaryocyte differentiation and platelet function
HDACs deacetylate histones
Pre NOTCH Transcription and Translation
Chromatin modifications during the maternal to zygotic transition (MZT)
Activated PKN1 stimulates transcription of AR (androgen receptor) regulated genes KLK2 and KLK3
Condensation of Prophase Chromosomes
RNA Polymerase II Promoter Opening
DNA methylation
SIRT1 negatively regulates rRNA expression
Assembly of the ORC complex at the origin of replication
0.0550
0.0575
0.0600
0.0625
GeneRatio
p.adjust
Count

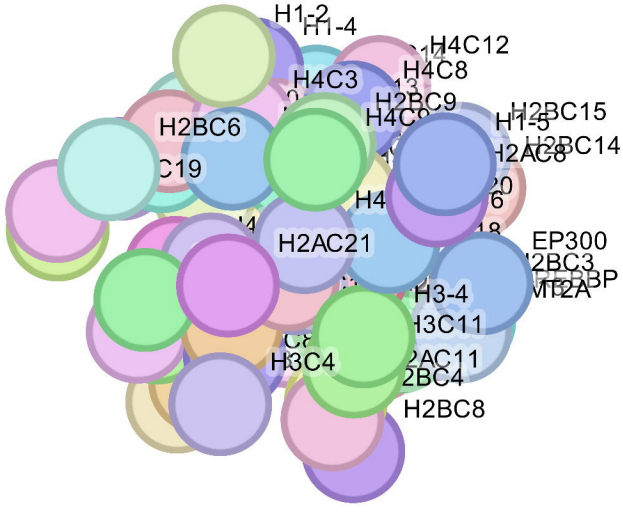
H1-2
H1-4
H4C12
H4C8
H4C3
H2BC9
H2BC15
H2BC6
H1-5
H2BC14
H2AC8
H2AC21
EP300
H3-4
H3C11
H3C4
H2BC8

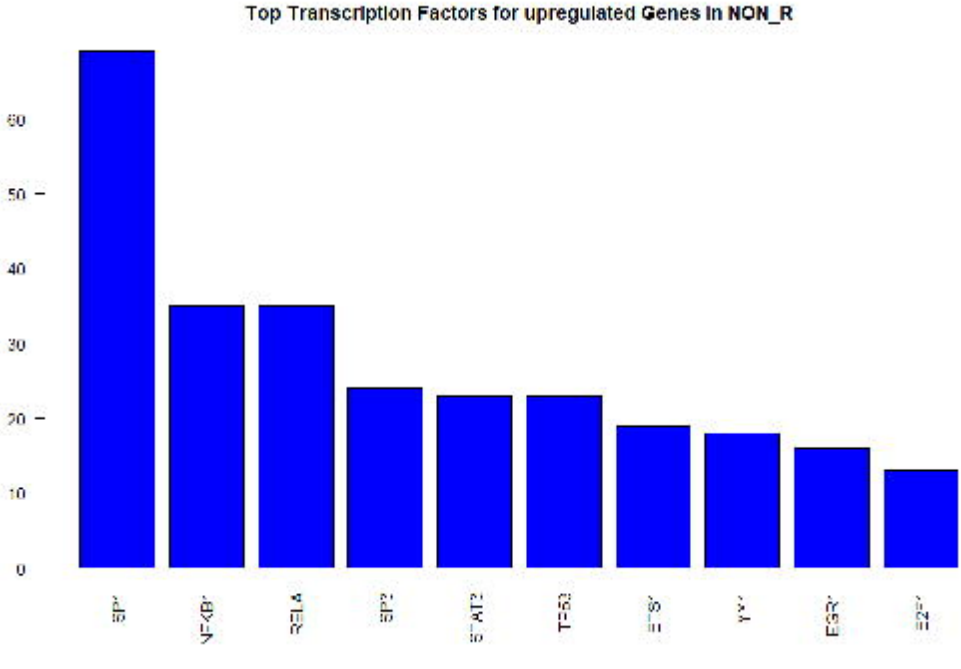
Top Transcription Factors for upregulated Genes in NON_R
60
50
40
30
20
10
0
SP1
NFKB1
RELA
SP2
STAT3
TP53
ETS1
YY1
ESR1
E2F1

TF–Target Network (Top 20 TFs)

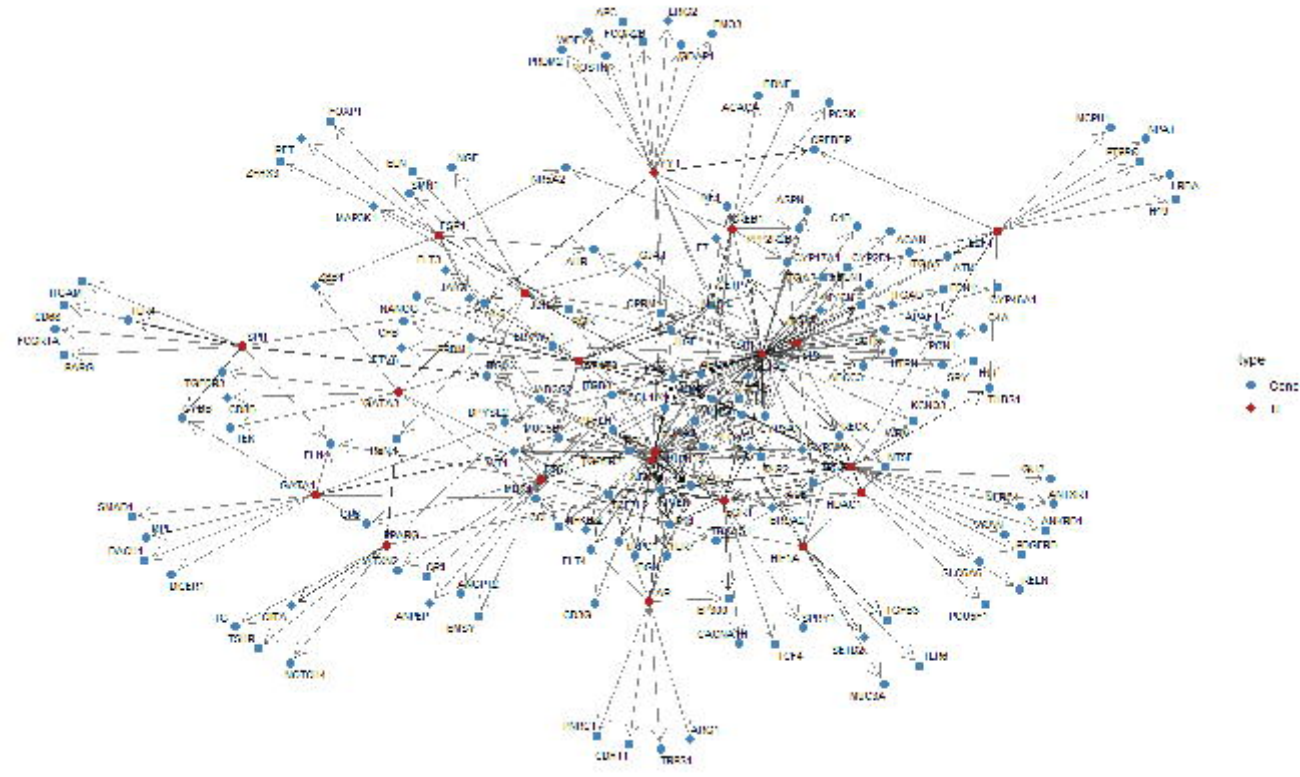

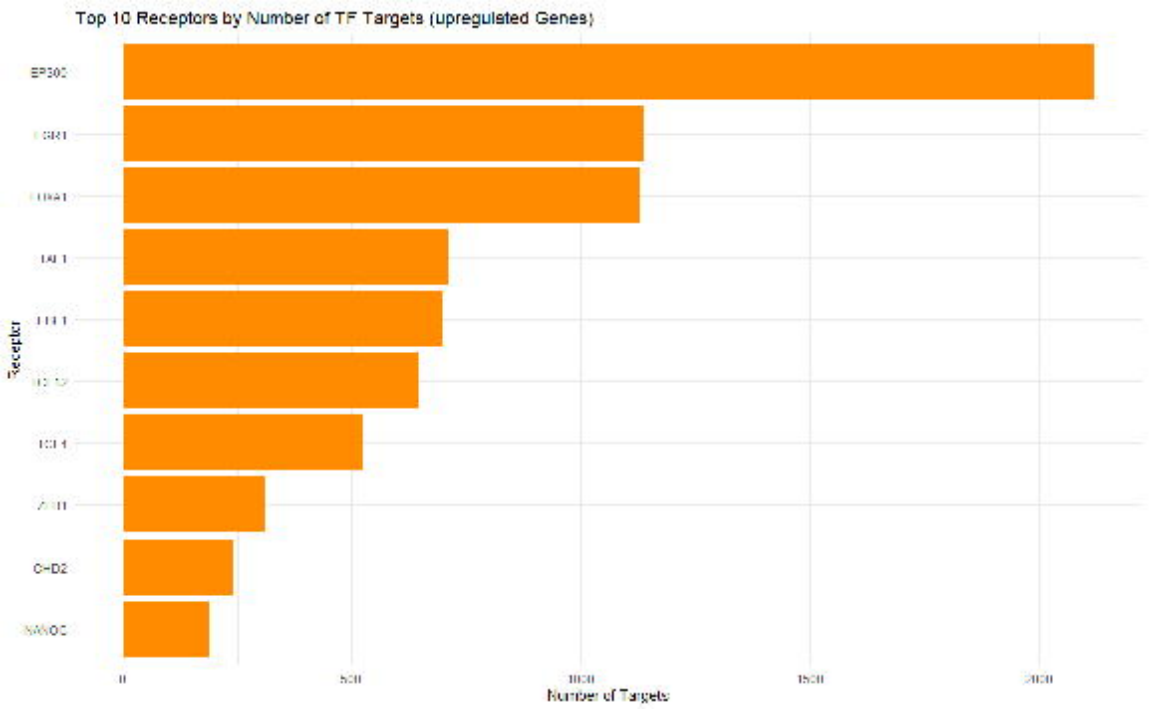
Top 10 Receptors by Number of TF Targets (upregulated Genes)
Receptor
Number of Targets

Top 20 Receptor–TF Network (upregulated Genes)

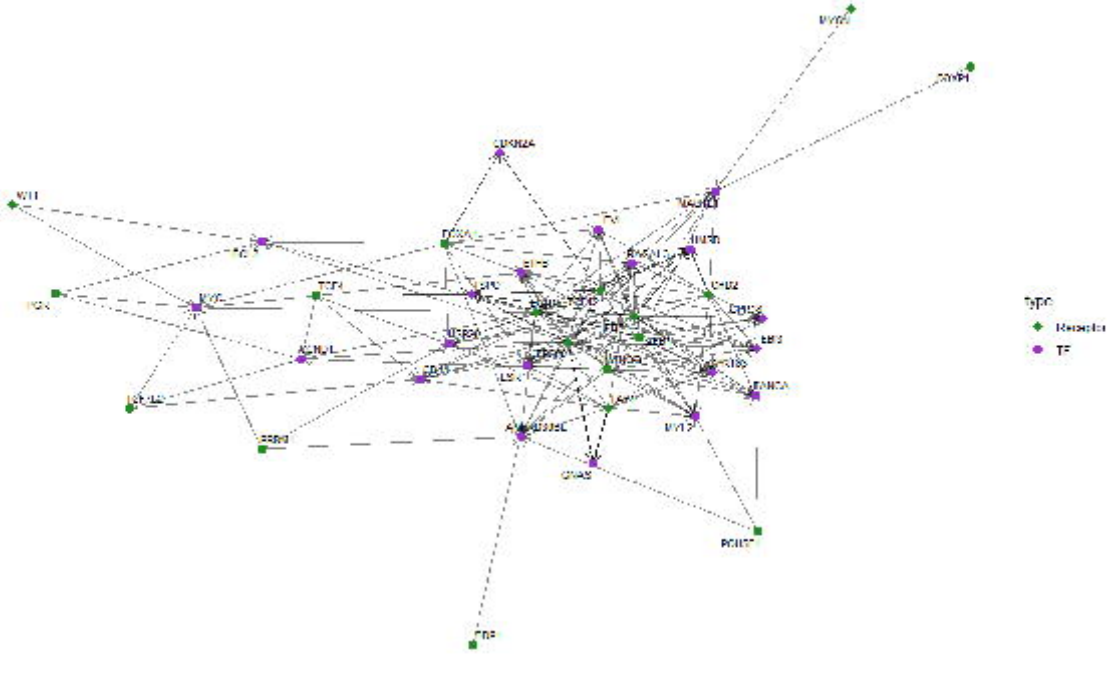
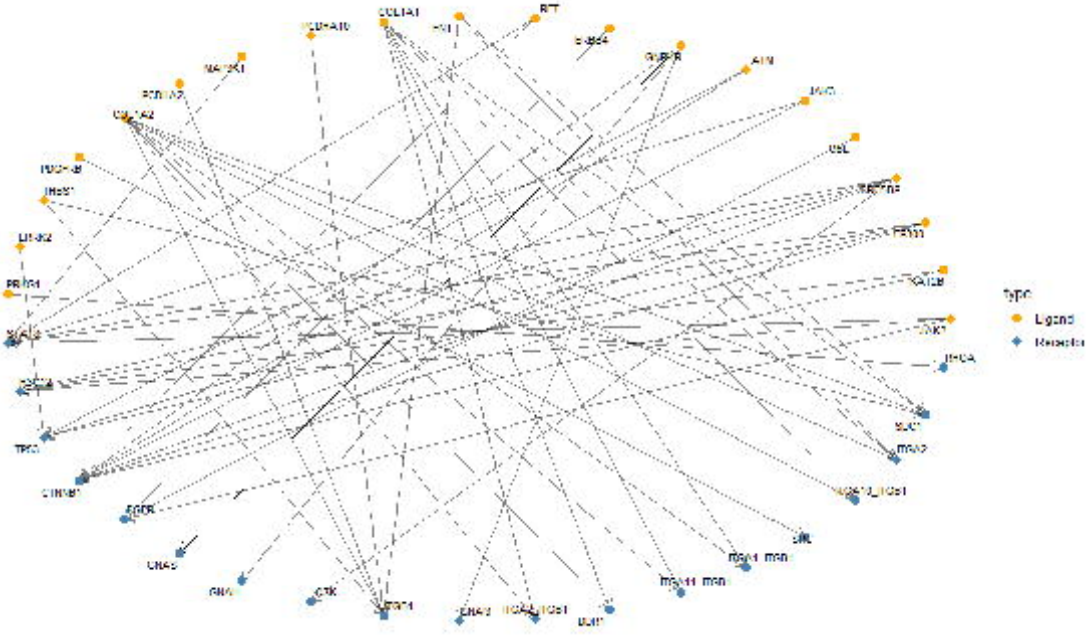
Top 20 Ligand−Receptor Network